Thin film morphologies of block copolymers with nanoparticles

Dieter Jehnichen,[1,a)] Doris Pospiech[1], Peter Friedel,[1] Guping He,[1] Alessandro Sepe,[2,b)] Jianqi Zhang,[2,c)] Christine M. Papadakis,[2] Rosa Taurino,[3] and Jan Perlich[4]

[1]*Leibniz-Institut für Polymerforschung Dresden e.V., Hohe Str. 6, D-01069 Dresden, Germany*
[2]*Technische Universität München, Physik Department, Fachgebiet Physik weicher Materie James-Franck-Str. 1, D-85748 Garching, Germany*
[3]*University of Modena and Reggio Emilia, Via Universita 4, I-41121 Modena, Italy*
[4]*Deutsches Elektronen-Synchrotron DESY, Notkestr. 85, D-22607 Hamburg, Germany*

Diblock copolymers (BCP) show phase separation on mesoscopic length scales and form ordered morphologies in both bulk and thin films, the latter resulting in nanostructured surfaces. Morphologies in thin films are strongly influenced by film parameters, the ratio of film thickness and bulk domain spacing. Laterally structured polymer surfaces may serve as templates for controlled assembly of nanoparticles. We investigated BCP of poly(n-pentyl methacrylate) and poly(methyl methacrylate) which show bulk morphologies of stacked lamellae or hexagonally packed cylinders. Thin films were investigated by atomic force microscopy and grazing-incidence small-angle X-ray scattering. For film thicknesses f well below d_{bulk}, standing cylinder morphologies were observed in appropriate molar ratios, while film thicknesses around and larger than d_{bulk} resulted in cylinders arranged parallel to surface. To alter and/or improve the morphology also in presence of different nanoparticles (NP: silica, gold), solvent vapour annealing (SVA) was applied. The BCP morphology usually remains unchanged but periodicities change depending on type and amount of incorporated NPs. It was found that silica clusters enlarge lateral distances of cylinders, whereas Au NPs reduce it. The effect of SVA is weak. The quality of morphology is slightly improved by SVA and lateral distances remain constant or are slightly reduced.

Keywords: X-ray scattering, block copolymers, phase separation, thin films, nanoparticles

a) Author to whom correspondence should be addressed. Electronic mail: djeh@ipfdd.de.
b) Actual Address: University of Cambridge, Department of Physics, Cavendish Laboratory, Madingley Road, Cambridge CB3 0HE, UK.
c) Actual Address: National Center for Nanoscience and Technology (NCNST), No.11 ZhongGuanCun BeiYiTiao, 100190 Beijing, P.R. China.

I. INTRODUCTION

Diblock copolymers (BCP) show phase separation on mesoscopic length scales and form ordered morphologies in both bulk and thin films resulting in nanostructured polymer surfaces (Benoit and Hadziioannou, 1988; Park *et al.*, 2003; Lazarri and López-Quintela, 2003; Segalman, 2005; Hamley, 2009; Kim *et al.*, 2010). In thin film geometry, the morphologies are strongly influenced by film parameters and the ratio of the film thickness and the bulk domain spacing (Krausch and Magerle, 2002; Knoll *et al.*, 2002; Albert and Epps, 2010). It is of high importance to understand these influences because laterally structured polymer surfaces may serve as template for the controlled assembly of nanoparticles (Nandan *et al.*, 2011).

In some BCP systems, for film thicknesses f well below d_{bulk} (the "repeat distance", which is controlled by the molar mass), standing morphologies were observed in appropriate molar ratios, while film thicknesses around and larger d_{bulk} resulted in structures arranged parallel to the surface (Fasolka and Mayes, 2001; Krausch and Magerle, 2002). In order to alter and/or improve the morphology - also in presence of different nanoparticles (NP, for example, silica, gold, silver, magnetite) - often solvent vapour annealing (SVA) was applied (Jehnichen *et al.*, 2010; Horechyy *et al.*, 2014).

The main goal of the present work is the creation of regularly ordered nanoparticle arrays by making use of the phase separation of the BCP in thin films as structural template for 1D (standing lamellae) and 2D (standing, hexagonally packed cylinders) morphologies, into which NPs can be incorporated selectively into one subphase.

The generation of such well-structured and stabile hybrid polymer/nanoparticle systems in thin films is demanding on both, chemistry and preparation. The first step is to find an appropriate block copolymer system with stable and reproducible morphology. Here, poly(*n*-pentyl methacrylate) - poly(methyl methacrylate) block copolymers (PPMA-*b*-PMMA) turned out to be well-suited (Jehnichen *et al*., 2008; Jehnichen *et al*., 2009; Pospiech *et al*., 2012). The specificity of this system is the all-methacrylic backbone allowing the easy removal of the BCP after templating. The synthesis of these BCP requires controlled polymerization methods. Sequential living anionic polymerization was proven as a suitable method (Keska *et al.*, 2006; Werner *et al.*, 2011). Temperature-dependent small-angle X-ray scattering in transmission (T-SAXS) was used to gather information about the bulk structure of BCP after synthesis, such as the type and the characteristic parameters of the ordered morphology, e.g. lamellar or hexagonally packed cylinders (Jehnichen *et al*., 2008; Werner *et al*., 2011). In addition, thin film preparation methods have to result in samples for advanced characterization with grazing-incidence small-angle X-ray scattering (GISAXS) experiments to investigate the presence of regular thin film morphologies of these block copolymers. The method of choice for BCP films was always dip-coating under controlled conditions.

The present work aimed at investigating the effect of different annealing procedures (temperature and solvent vapour annealing, as reported in Sepe *et al*. (2014) and Zhang *et al*. (2014)) on the improvement of the morphology.

Incorporation of nanoparticles into the polymer matrix is probably the most important step of nanoparticle array preparation. Nanoparticles were either formed *in–situ* in the BCP film by a sol-gel process according to (Taurino, 2008; Fischer *et al.*, 2008) yielding silica NP, or, on the other hand, by adding pre-formed NPs (here: Au NPs) to the BCP solution before dip coating. Both techniques are regarded as possibility to insert nanoparticles well-directed to one phase of the block copolymer morphology. Figure 1 illustrates the goal and workflow of the present study.

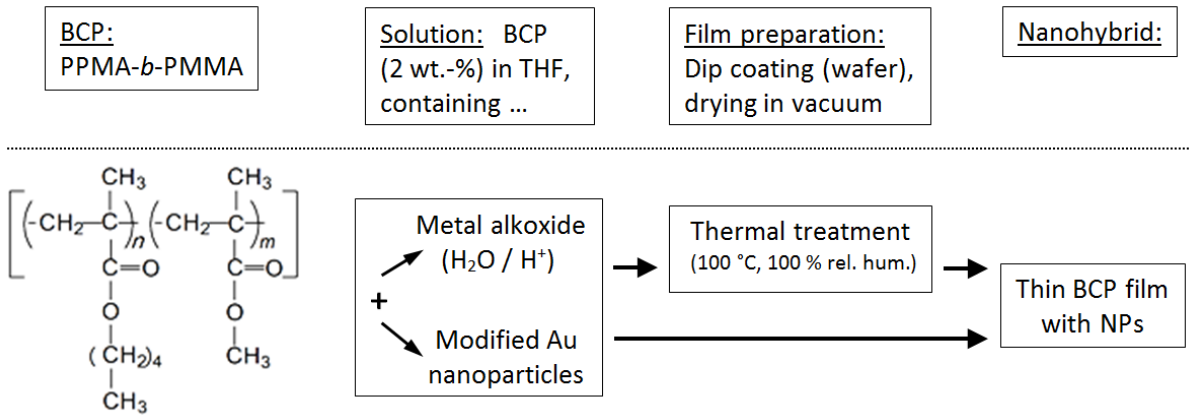

Figure 1. Schematic representation of the steps for achieving block copolymer/nanoparticle hybrids with PPMA-*b*-PMMA block copolymers in both applied preparation procedures.

Pre-characterizations of the materials and thin films were carried out using T-SAXS and X-ray reflectometry (XRR). Characterization of the thin film samples as well as the structural changes after an online or offline sample annealing was realized in GISAXS experiments (for methodical details see, e.g., Müller-Buschbaum (2003), Müller-Buschbaum (2009), Jehnichen *et al*. (2013)) and atomic force microscopy (AFM) investigations. Moreover, the influence of the incorporated NPs onto the morphology of selected PPMA-*b*-PMMA was investigated.

II. EXPERIMENTAL

A. Sample preparation

1. Synthesis

a) The PPMA-*b*-PMMA diblock copolymers used in this study were synthesized by sequential living anionic polymerization in THF/LiCl at -78 °C using *sec*-butyl lithium/diphenyl ethylene as initiator as reported earlier (Keska *et al.*, 2006; Werner *et al.*, 2011) aiming at narrow polydispersity (~1.1). The averaged molar masses M_w and M_n were determined by SEC yielding values relative to narrowly distributed PMMA standards. The samples employed in this work are listed in TABLE I.

TABLE I. Diblock copolymers PPMA-*b*-PMMA under investigation – chemical composition, molar masses, structure parameters of bulk morphology (T-SAXS) and thin films parameters from XRR and AFM (samples without NPs); all parameters are rounded.

Sample	**Molar mass** M_w (g/mol)	**Molar ratio** n/m*	**Bulk morphology**** d_{100} (nm)	a_{hex} (nm)	**Film thickness** f_{XRR} (nm)	**Film morphology***** (from AFM)
PM13	54,000	72/28	38.3	44.2	20	lying + few[1] standing HPC
PM70	184,000	70/30	49.8	57.5	40	standing HPC
PM67	193,000	71/29	57.8	66.7	20	lying HPC[2]
PM69	407,000	82/18	66.0	76.2	43	lying HPC[2]

* Assignment according to Figure 1.

** After heating/cooling cycle to 200 °C; HPC: hexagonally packed cylinders.
*** After dip-coating and subsequent drying at room temperature in vacuum.
[1] Amount of standing HPC is increased for higher content of Au nanoparticles.
[2] Film without silica nanoparticles (before TEOS treatment).

b) The Au nanoparticles (Au18) with an average core diameter of 2 nm (Figure 2) were prepared by the Brust-Schiffrin method (Brust *et al.*, 1994) and were stabilized with dodecanethiol (Yee *et al.*, 1999).

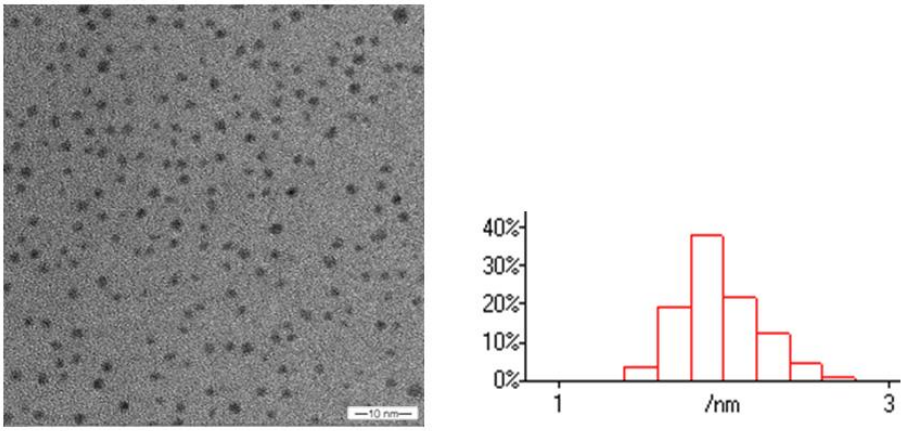

Figure 2. (Colour online) a) Transmission electron microscopy (TEM) image (magnification: 400,000 x, scale bar: 10 nm) and b) nanoparticle size distribution of dodecanthiol-stabilized Au NP (Au18) with a mean core diameter of 2 nm.

2. Film preparation

Thin films of BCP were applied by dip-coating of Si wafers pre-cleaned by piranha solution at 80 °C for 0.5 h, followed by thoroughly rinsing with deionized water and drying with pressurized nitrogen.
Au NP containing films: Pre-cleaned Si wafers were dip-coated by dilute BCP solutions (pure or with different contents of modified Au NPs) in tetrahydrofuran (THF). Subsequently, the wafers were dried at room temperature in a vacuum oven.
Off-line SVA was performed with THF (in saturated vapour for 1 h, followed by drying for 5 h in air, both at room temperature).
For silica NPs, an off-line procedure for the generation of silica inside the already prepared thin film was used. The films were prepared as described above by dip-coating. The in-film generation of silica NP (Fischer *et al.*, 2008; Yuan *et al.*, 2008) was performed by treating the thin BCP films in three steps as follows: The films were stored in tetraethoxysilane (TEOS) saturated vapour over 24 h, than in H_2O/HCl (9:1) saturated vapour for 10 h, and afterwards annealed for 2 h at 100 °C in vacuum.

B. X-ray scattering experiments and AFM

1. T-SAXS

Temperature-dependent small-angle X-ray scattering was carried out at the Soft Condensed Matter Beamline BW4 (Roth *et al.*, 2006; HASYLAB @ DESY Hamburg, λ_{BW4} = 0.138 nm) using a MarCCD 165 area detector (Marresearch Inc., USA). Oven experiments between room temperature and 200 °C were performed using heating/cooling rates of 3 K/min.

2. XRR and GISAXS

X-ray reflectometry (XRR) was performed using a diffractometer XRD T/T (GE Inspection Technologies Ahrensburg, Germany) in symmetric step-scan mode with $\Delta 2\Theta$ = 0.01° and t = 3 s (Cu $K\alpha$ radiation) for pre-examination of few film parameters (e.g., film thickness).
Grazing-incidence small-angle X-ray scattering (GISAXS) was carried out at the Beamline BW4 (Roth *et al.*, 2006; HASYLAB @ DESY Hamburg, λ_{BW4} = 0.138 nm) using a MarCCD 165 area detector (Marresearch Inc., USA). 2D-patterns with incidence angles α_i = 0.03° - 0.30°, i.e. close to the critical angles α_c (polymer film, e.g., pure PMMA: $\alpha_{c,BCP} \approx 0.148°$; substrate SiO_x: $\alpha_{c,SiOx} \approx 0.20°$), were accumulated with sufficiently high measuring time (typically 150 s) to find an optimal value α_i so the lateral coherent scattering was most pronounced. This turned out to be the case for $\alpha_i = 0.18° > \alpha_{c,BCP}$.

3. Microscopic investigations

Transmission electron microscopy (TEM) investigations to measure the size of Au NPs were performed by means of a transmission electron microscope LIBRA 120 at IPF Dresden. At this, the nanoparticle dispersion was dropped on a TEM copper grid and after drying.
Atomic force microscopy (AFM) measurements before and/or after film treatment and GISAXS experiments, respectively, were done with the scanning force microscope NanoScope IIIa-D3100 (Digital Instruments) in tapping mode. The mean lateral distances L_0 from the PSD (power spectral distribution) obtained by FFT of the AFM image were calculated using the related AFM software.

III. RESULTS AND DISCUSSION

A. Bulk behaviour

All PPMA-*b*-PMMA BCP samples employed in the study showed morphologies with hexagonally packed cylinders. Three of them had a molar ratio PPMA/PMMA of 70/30 mol/mol, for which the hexagonal morphology is expected (TABLE 1), but also the very asymmetric sample PM69 with a molar ratio of 82/18 mol/mol displayed this morphology. Figure 3a-d illustrates the scattering curves of the bulk material after a complete heating/cooling cycle starting from the as-synthesized state. Based on the position of the first scattering maximum, q_1, and the known ratios of the next allowed reflections q_1/q_n of the hexagonally packed cylinder morphology (HPC) (i.e. 1 : √3 : √4 : √7 : √9 …), the expected positions of the higher order reflections were calculated (see Figure 3a-d). This way, a HPC morphology could be identified for all samples. The corresponding morphology parameters, namely the lattice spacings (d_{100}) and corresponding cylinder-cylinder distances, a_{hex} (unit cell parameter of HCP), are given in TABLE I.

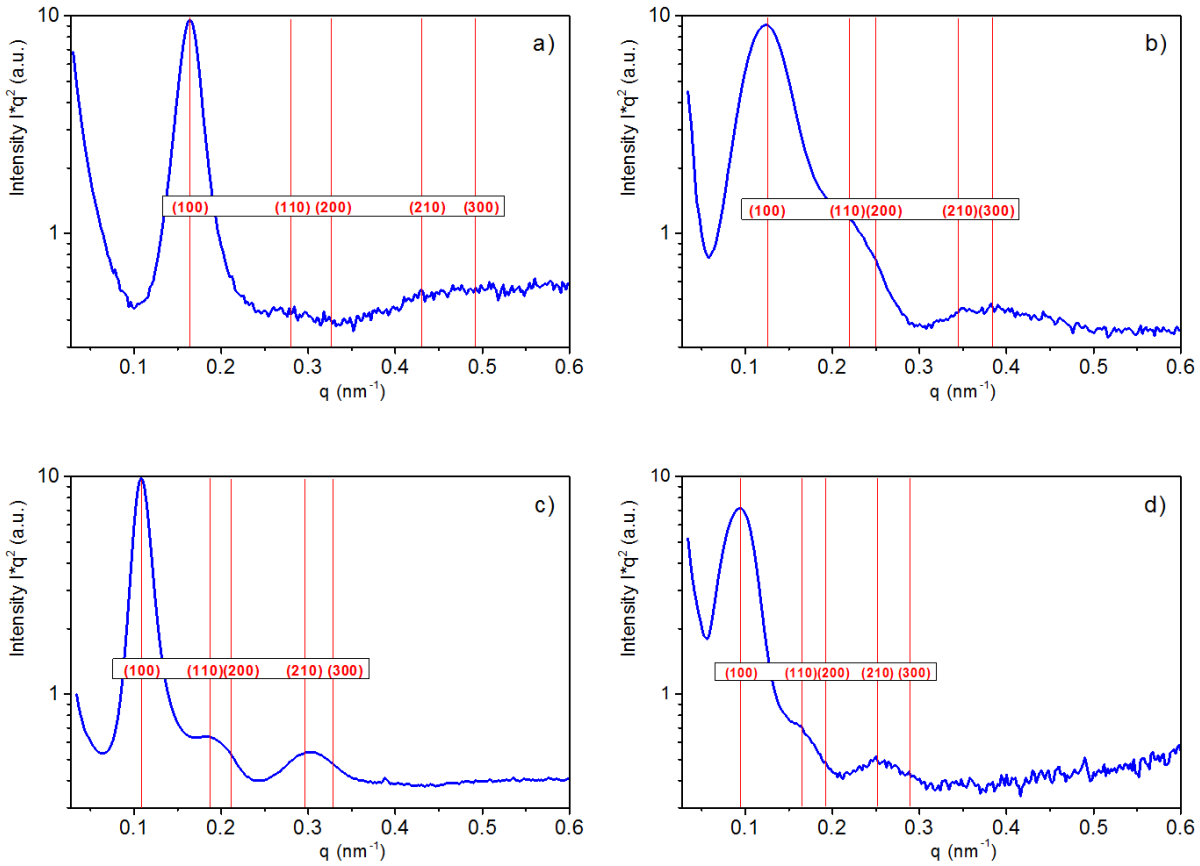

Figure 3. (Colour online) Lorentz-corrected SAXS-curves of corresponding BCP bulk material with HCP morphology (with Miller indexing of the first reflections (hk0)). (a) PM13, (b) PM70, (c) PM67, (d) PM69.

B. Thin films

1. XRR and AFM

For determination of the film thickness, pre-evaluation of the film roughness and direct visualization of the thin film morphology XRR and AFM investigations were performed prior to GISAXS experiments. As-prepared films (film thicknesses f_{XRR} ranging from 20 to 43 nm) show distinct Kiessig interferences, low roughness (typical rms-roughnesses 0.7-0.8 nm) and good preparation reproducibility. The AFM images give a direct impression of the morphology in the topmost layer of the thin film (see for example Figure 5). Film parameters obtained by XRR and AFM are summarized in TABLE I.

2. GISAXS results and film treatment

2.1. BCP films with Au nanoparticles

In a first sample series the results of film preparation from the appropriately diluted BCP/Au NP solution with different amount of nanoparticles were compared. The Au NPs (Au18 with an average core diameter of 2 nm) are surface modified with dodecane thiol. The alkyl rest is hydrophobic and the preferential interaction with the pentyl methacrylate block should direct the NPs into the PPMA phase. The GISAXS results for PM13 films with low and medium content of Au18 NPs in comparison with the pure BCP film and one test of offline SVA (BCP film with 5 wt.-% Au NPs) are given in Figure 4a-d. It shows the influence of the amount of Au NP and SVA, respectively, on the laterally ordered morphology. Besides scattering experiments, AFM measurements were carried out and evaluated by means of PSD (Figure 5a-d).

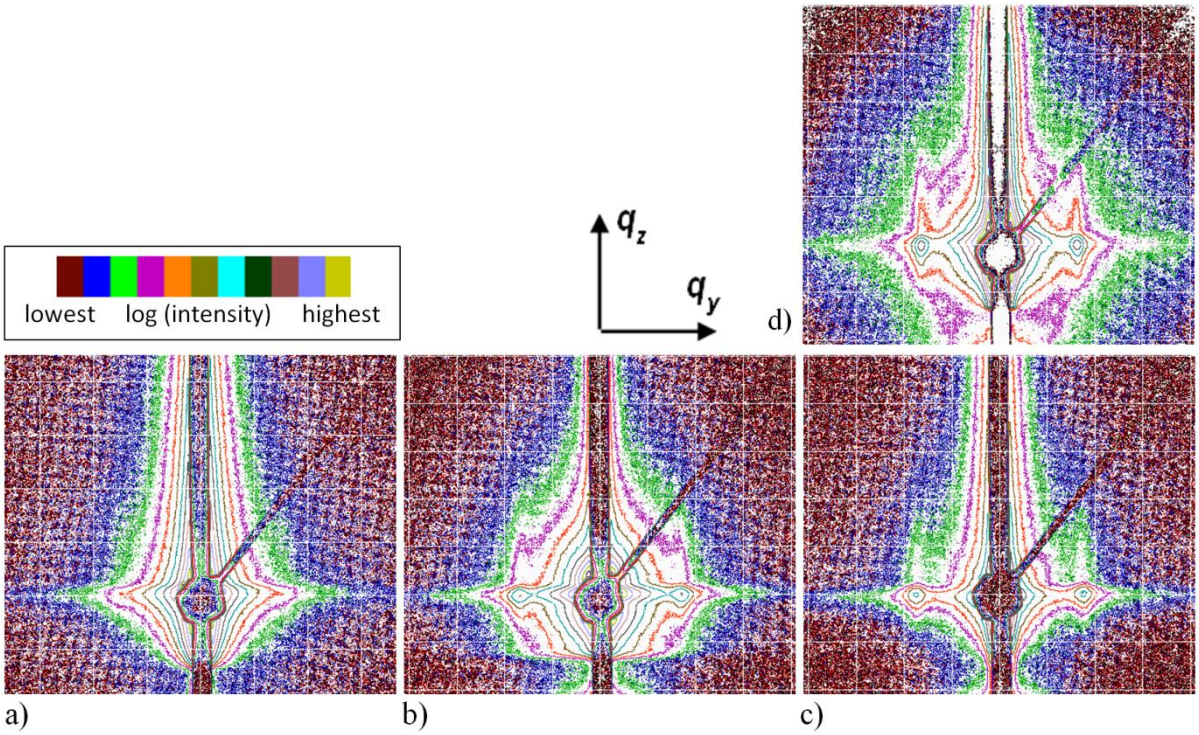

Figure 4. (Colour online) 20 nm films of sample PM13/Au18 *vs*. concentration of NP [a), b), c), d): 0, 1, 5, and 5 wt.-%] and influence of SVA with THF [a) - c) as spin-coated, d) vapour-annealed]. GISAXS pattern, scattering intensity plot (in miscolour) log(*I*) *vs*. q_z,q_y (q_z range: approx. 0.08 … 0.78 nm^{-1}, q_y range: approx. -0.40 … 0.40 nm^{-1}, mesh size Δq = 0.1 nm^{-1}).

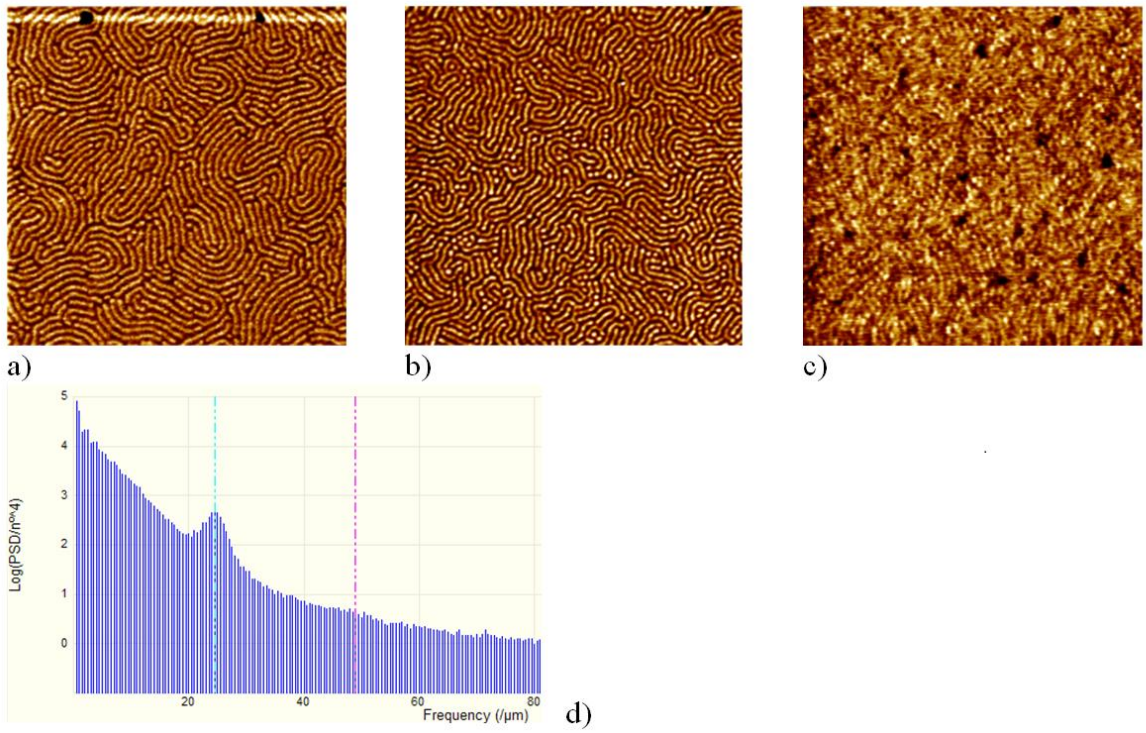

Figure 5. (Colour online) AFM results from 20 nm films of sample PM13/Au18 *vs*. concentration of NP [a), b), c): 0, 1, and 5 wt.-%; as spin-coated]. AFM phase contrast images (pattern size 2×2 μm^2, scale 3°); d) PSD of FFT image of AFM image a). (L_0 is the result from reading of the peak position).

In comparison to the pure BCP film morphology, the lateral distance of cylinders is reduced with increasing content of NPs in the case of the small Au NPs (core diameter of 2 nm) used in the present study. This behaviour differs from the case of significantly larger Au NPs (average core diameter of ~10 nm) (He, 2014) where it was found that the required space of these larger NPs perturbs the morphology. However, SVA of the sample with 5 wt.-% small Au NPs enlarges the lateral distance. From this change in the repeat distances we conclude that the Au NPs after SVA are located either in the PMMA domain or at the interface between the PPMA and the PMMA domains. The latter scenario can be ruled out due to the fact that the repeat distance shrinks when the NPs are at the interface because the interfacial tension is reduced (He, 2014). The third possibility - equal distribution of Au NPs within the film - can be excluded because of the strong enhancement of the reflections when Au NPs are added (Figure 6) in comparison to the pure BCP film.

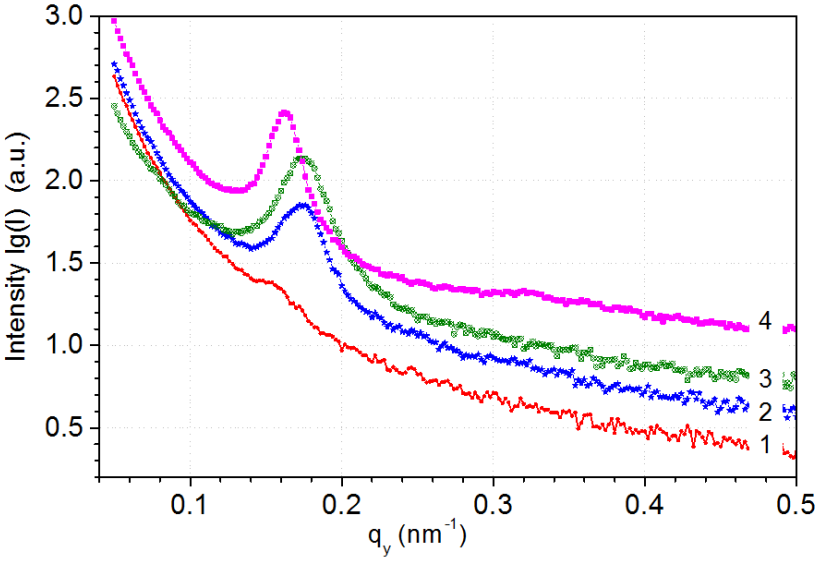

Figure 6: (Colour online) GISAXS results from 20 nm films of sample PM13/Au18 *vs.* concentration of NPs [(1), (2), (3): 0, 1, and 5 wt.-%) and influence of SVA with THF (4) for film with 5 wt.-% Au NPs]. Out-of-plane curves from the GISAXS patterns (Figure 4a-d), taken at $q_z = q_{Yoneda,BCP}$.

TABLE II. Hybrid thin films of BCP PM13 with Au18 NPs – thin film parameters and effect of SVA (L_0 from AFM, GISAXS d values found at $\alpha_i = 0.20°$; all parameters are rounded).

Lateral film structure	**AFM**	**GISAXS***	
	L_0 (PSD) (nm)	d_{100} (nm)	a_{hex} (nm)
Concentration of Au NP:			
0 wt.-%	40.8	39.9	46.0
1 wt.-%	39.2	35.7	41.2
5 wt.-%	38.5	35.8	41.3
5 wt.-% + vapour ann.	--	38.3	44.2

* GISAXS shows often only one broad lateral correlation peak (set as d_{100}). a_{hex} – unit cell parameter, derived from d_{100}; problematical in case of mixed arrangements of lying and standing cylinders (Lee *et al.*, 2005).

The position of the lateral correlation peak (TABLE II) does not scale with the amount of NPs. From the AFM image (Figure 5a-c), it can be concluded that lying parallel cylinders in the BCP film without NPs switch to a mix of both lying and standing (perpendicular) cylinders and an amount of randomly

oriented ones when Au NPs were incorporated. The amount of standing cylinders increased with the concentration of Au NPs.
The orientational switch of the nanodomains can be explained by the altered interaction of the BPC with the substrate due to modified Au NPs. In the pure BCP, the hydrophilic PMMA block tends to wet the substrate partially, resulting in lying cylinders. When Au NPs are present and assemble selectively in the PMMA domains, the PMMA cylinders become more hydrophobic, thus they reduce their contact with the substrate, which result in standing cylinders.
An additional SVA with the non-specific solvent THF of the BCP film containing 5 wt.-% Au NPs resulted in a lateral improvement of the thin film morphology (i.e. in sharper reflections) as well as along the film normal, as seen from the enhanced Bragg rods in the GISAXS pattern (compare Figures 4c and 4d). The reason is probably that THF is a non-selective, good solvent for both blocks which enhance the polymer mobility in the swollen state which allow structural rearrangements. On the other side, a generation of thin layers of Au NPs near the film surface or near the substrate surface cannot be excluded absolutely. The increased background of the out-of-plane curves (4) in Figure 6 (BCP film with 5 wt.-% Au NPs after SVA treatment) could follow from such NP enrichments.

2.2. BCP films with silica nanoparticles

In a second sample series, it was investigated whether silica nanoparticles can be generated by TEOS treatment of a previously prepared nano-patterned BCP thin film. The treatment is based on the interaction of the silica precursor TEOS with the film surface over different treatment steps. The actual content of silica cannot be determined after such a procedure. The results of the treatment steps were monitored by offline GISAXS measurements (as an example: see Figure 7a-d).

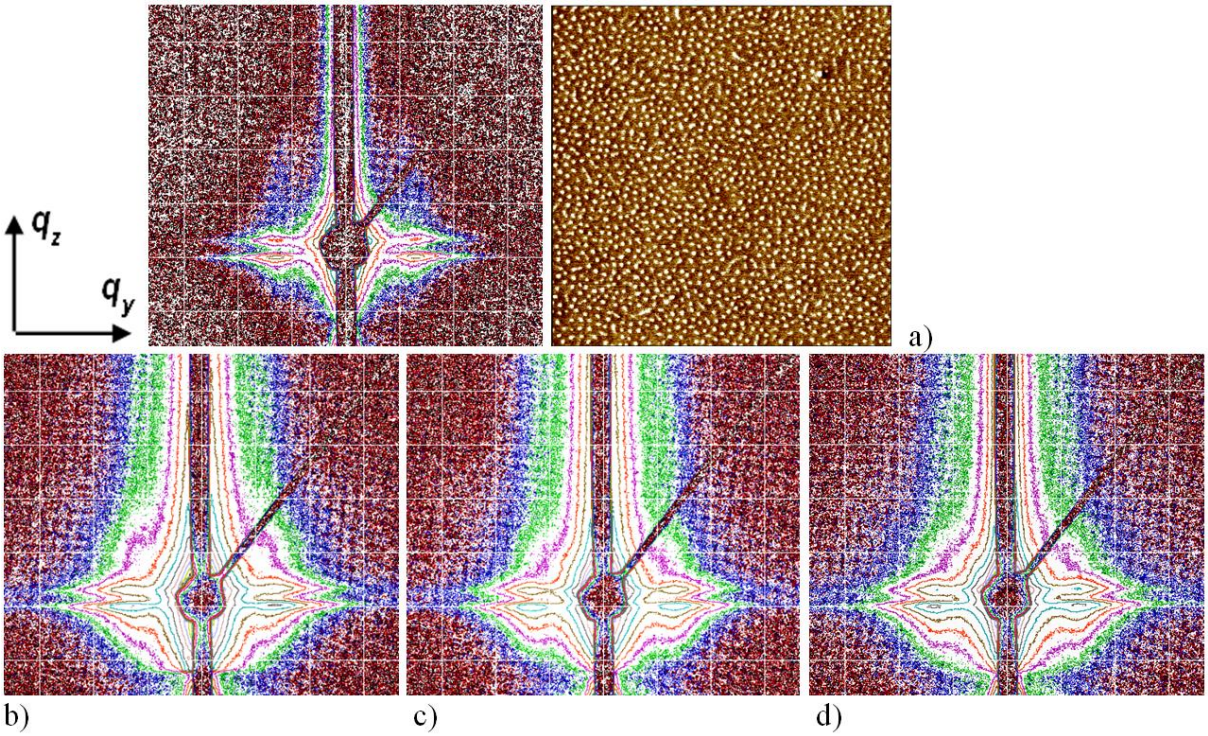

Figure 7. (Colour online) GISAXS patterns of 40 nm thick films of sample PM70 after offline TEOS treatment (generation of SiO_2 NPs). a) as coated, b) after treatment with TEOS vapour, c) after treatment with H_2O/HCl vapour, d) after annealing at 100 °C in vacuum. Scattering intensity plot (in miscolour) log(*I*) *vs*. q_z,q_y (q_z range: approx. 0.12 … 0.75 nm^{-1}, q_y range: approx. -0.36 … 0.36 nm^{-1}, mesh size Δq = 0.1 nm^{-1}). Additionally in a), an AFM phase contrast pattern is shown (pattern size 2×2 μm^2, scale 3°).

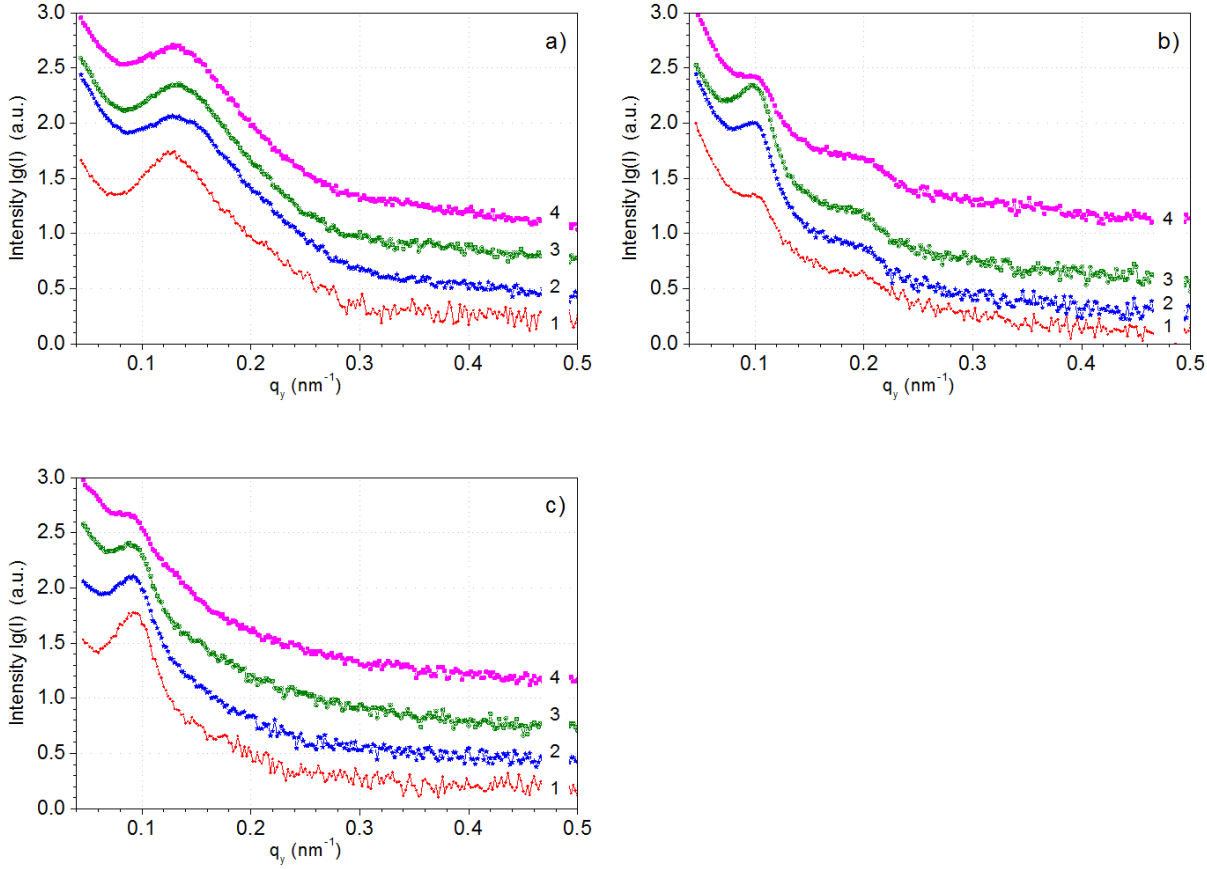

Figure 8. (Colour online) Thin films of samples a) PM70, b) PM67, and c) PM69: Out-of-plane curves from GISAXS patterns at $q_z = q_{Yoneda,BCP}$ after offline TEOS treatment [(1) as coated, (2) after treatment with TEOS vapour, (3) after treatment with H_2O/HCl vapour, (4) annealed at 100 °C in vacuum], curves are shifted vertically for clarity. Corresponding 2D GISAXS patterns are given in Figure 7a-d at the example of sample PM70.

For the BCPs PM70, PM67 and PM69, the out-of-plane intensity profiles of the corresponding GISAXS patterns after each treatment step are compared in Figure 8a-c. In the nanohybrids under investigation, the type of morphology remains the same as in the pure BCP. For all treatment steps shown in Figures 7 and 8, a lateral arrangement of standing cylinders with hexagonal packing over a certain correlation length is found. However, there are differences when comparing the quality of lateral correlation of the cylinders in the three different BCPs. PM67 with a film thickness of only 20 nm and the largest ratio a_{hex}/f (i.e. ratio of domain size to film thickness) shows the best ordered HPC morphology due to lower peak widths and presence of higher order reflections. Moreover, from the enhancement of the correlation peak intensity during the TEOS treatment, we conclude that silica particles are selectively generated in the PMMA cylinders. In contrast, the thin films of both PM70 and PM69 (film thickness ~40 nm) feature a significantly lower quality of HCP morphologies. Moreover, contrary to PM67, the intensity of the reflection decreases during the TEOS treatment. From this, it can be concluded that the generation of silica takes place in both, the PMMA and the PPMA domains. After the in-situ generation of silica NPs only weak changes of lateral distances are found, such as an increase of about 2.2 nm (PM69) or a reduction of about 2.5 nm (PM70), or no change (PM67) (compare TABLE III).

TABLE III. Silica generation in PPMA-*b*-PMMA films – thin film parameters after treatment (GISAXS: *d* values found at $\alpha_i = 0.20°$; all parameters are rounded).

Sample	**PM70**		**PM67**		**PM69**	
Lateral film structure*	d_{100} (nm)	a_{hex} (nm)	d_{100} (nm)	a_{hex} (nm)	d_{100} (nm)	a_{hex} (nm)
Treatment:						
as-coated	48.0_b	(55.4)	61.2	70.7	66.2	76.5
+ TEOS	45.0_b	(52.0)	61.4	70.9	66.9	(77.2)
+ H_2O/HCl	45.0_b	(52.0)	61.5	71.0	67.5	(78.0)
+ *T* =100 °C	45.5_b	(52.5)	61.3	70.8	67.5	(78.0)
Tendency	weak decrease		~ constant		weak increase	

$_b$ Broad reflection.

* Following the morphology found by AFM as HPC, regardless of details in lateral intensity distribution of GISAXS (often only one broad peak, which was used to determine d_{100}). a_{hex} – unit cell parameter, derived from lateral correlation peak.

It has previously been shown by us that functionalization of the PMMA blocks by -OH end groups resulted in BCP that worked well as a template for the formation of silica NPs by TEOS treatment (Werner *et al.*, 2011). From the GISAXS experiments (Figure 7 and 8), it can be concluded that the off-line silica generation caused also an enhancement of the diffuse scattering due to the increased background of the out-of-plane curves (having the highest values after the last treatment step). Moreover, a defined amount of randomly oriented cylinders cannot be excluded.

IV. CONCLUSION AND OUTLOOK

In addition to the structures expected from the bulk morphologies, thin film structures of BCP are characterized by the geometric confinement resulting in orientation effects which depend on the ratio between the film thickness and the bulk domain spacing. The present investigation demonstrates that two routes to prepare nano-patterned thin diblock copolymer thin films based on PPMA-*b*-PMMA with nanoparticles allow us to obtain thin films in a range of film thicknesses having low roughness and good reproducibility. These preparation routes are dip-coating of Si wafers with dilute solutions of BCP and NPs and off-line treatment of previously prepared, pure BCP films with vapour containing a precursor of the final NPs. In the nanohybrids under investigation (PPMA-*b*-PMMA BCPs with Au and silica NPs), the type of morphology remains similar to the one in the pure BCP film. The dimensions of the lateral film morphology depend weakly on type and amount of incorporated NPs as well as on the molar mass and the composition of the BCP. For the examined sample systems, it can be stated that silica NPs can lead to both an increase and a decrease of the lateral distance of the PMMA cylinders. On the other hand, metallic nanoparticles often lead to a decrease of the domain spacing (confirmed here for the case of small Au NPs). This result is in accordance with the result found by Horechyy *et al.* (2014). In the present system, an enrichment of NPs in the surface region is not observed, but cannot be excluded either because of the presence of diffuse scattering in case of generated silica NPs. More detailed X-ray scattering investigations, especially for off-line generation of silica NPs, have to be performed to clarify the effects of constrained dimensions onto the morphology variation in thin films with altered film thickness, but still smaller than the domain spacings.

ACKNOWLEDGEMENTS

We gratefully acknowledge financial support by and participation in EU NoE "NANOFUN-POLY". We thank HASYLAB @ DESY Hamburg (now: DESY Photon Science) for providing beamtime and offering excellent equipment. Moreover, we thank all not-named colleagues of the IPF participating in synthesis and characterization of the studied polymers. Special thanks go to Kathrin Eckstein for anionic polymerization and Andreas Korwitz for excellent assistance during the GISAXS experiments, especially during the TEOS treatment.

REFERENCES

Benoit, H., and Hadziioannou, G. (**1988**). "Scattering theory and properties of block copolymers with various architectures in the homogeneous bulk state", *Macromolecules* **21**, 1449 - 1464.

Brust, M., Walker, M., Bethell, D., Schiffrin, D. J., and Whyman, R. (**1994**). "Synthesis of thiol-derivatised gold nanoparticles in a two-phase Liquid–Liquid system", *J. Chem. Soc., Chem. Commun.* **7**, 801 - 802.

Fasolka, M. J., and Mayes, A. M. (**2001**). "Block Copolymer Thin Films: Physics and Applications ", *Annu. Rev. Mater. Res.* **31**, 323 –355.

Fischer, D., Pospiech, D., Scheler, U., Navarro, R., Messori, M., and Fabbri, P. (**2008**). „Monitoring of so-gel synthesis of organic-inorganic hybrids by FTIR transmission FTIOR/ATR, NIR and Raman spectroscopy", *Macromol. Symp.* **265**, 134 - 143.

He, G. (**2014**). "The Effect of Modified AuNPs on the Morphology and Nanostructure Orientation of PPMA-b-PMMA Block Copolymer Thin Films", PhD Thesis, Technische Universität Dresden (Germany), (submitted).

Horechyy, A., Nandan, B., Zafeiropoulos, N. E., Jehnichen, D., Göbel, M., Stamm, M., and Pospiech, D. (**2014**). „Nanoparticle directed domain orientation in thin films of asymmetric block copolymers", *Colloid Polym. Sci.* **292**, (online 05/2014, http://dx.doi.org/10.1007/s00396-014-3251-7).

Jehnichen, D., Pospiech, D., Keska, R., Ptacek, S., Janke, A. Funari, S. S., Timmann, A., and Papadakis, C. M. (**2008**). „Analysis of thin nanostructured block copolymer films by GISAXS and AFM", *J. Nanostruct. Polym. Nanocomp.* **4**, 119 - 128.

Jehnichen, D., Pospiech, D., Ptacek, S., Eckstein, K., Friedel, P., Janke, A., and Papadakis, C. M. (**2009**). „Nanophase-separated diblock copolymers: Structure investigations on PPMA-*b*-PMMA using X-ray scattering methods", *Z. Kristallogr. Suppl.* **30**, 485 - 490.

Jehnichen, D., Pospiech, D., Friedel, P., Korwitz, A., Berndt, A., Janke, A., Näther, F., Papadakis, C. M., Sepe, A., and Perlich, J. (**2010**). „Structure investigations in thin films of poly(pentyl methacrylate-*b*-methyl methacrylate)s and their nanocomposites with nanoparticles", *HASYLAB Annual Report*, 20101160, PhotonScience@DESY Hamburg (http://photon-science.desy.de/annual_report/files/2010/20101160.pdf).

Jehnichen, D., Pospiech, D., Friedel, P., and Funary, S. S. (**2011**). „Semifluorinated PMMA/PSFMA diblock copolymers with multiple phase separation", *Z. Kristallogr. Proc.* **1**, 487 - 492.

Jehnichen, D., Friedel, P., Selinger, R., Korwitz, A., Wengenmayr, M., Berndt, A., and Pospiech, D. (**2013**). "Temperature dependant structural changes in thin films of random semifluorinated PMMA copolymers", *Powder Diffr.(Suppl.)* **28**, 144 – 160.

Keska, R., Pospiech, D., Eckstein, K., Jehnichen, D., Ptacek, S., Häußler, L., Friedel, P., Janke, A., and Voit, B. (**2006**). "Study of the phase behavior of poly(pentyl methacrylate-*b*-methyl methacrylate) diblock copolymers", *J. Nanostruct. Polym. Nanocomp.* **2**, 43 - 52.

Kim, H.-C., Park, S.-M., and Hinsberg, W. D. (**2010**). „Block copolymer based nanostructures: materials, processes, and applications to electronics", *Chem. Rev.* **110**, 146 - 177.

Knoll, A., Horvat, A., Lyakhova, K. S., Krausch, G., Sevink, G. J. A., Zvelindovsky, A. V., and Magerle, R. (**2002**). "Phase behavior in thin films of cylinder-forming block copolymers", *Phys. Rev. Lett.* **89**, 0355011 - 0355014.

Krausch, G., and Magerle, R. (**2002**). „Nanostructured thin films via self-assembly of block copolymers", *Adv. Mat.* **14**, 1579 - 1583.

Lazzari, M., and López-Quintela, M. A. (**2003**). "Block copolymers as a tool for nanomaterial fabrication", *Adv. Mater.* **15**, 1583-1594.

Lee, B., Park, I., Yoon, J., Park, S., Kim, J., Kim, K.-W., Chang, T., and Ree, M. (**2005**). "Structural Analysis of Block Copolymer Thin Films with Grazing Incidence Small-Angle X-ray Scattering", *Macromolecules* **38**, 4311 - 4323.

Hamley, I. W. (**2009**). "Ordering in thin films of block copolymers: Fundamentals to potential applications", *Progr. Polym. Sci.* **34**, 1161 – 1210.

Müller-Buschbaum, P. (**2003**). "Grazing incidence small-angle X-ray scattering: an advanced scattering technique for the investigation of nanostructured polymer films," *Anal. Bioanal. Chem.* **376**, 3 – 10.

Müller-Buschbaum, P. (**2009**). "A Basic Introduction to Grazing Incidence Small-Angle X-Ray Scattering," *Lect. Notes Phys.* **776**, 61 – 89.

Nandan, B., Kuila, B. K., and Stamm, M. (**2011**). „Supramolecular assemblies of block copolymers as templates for fabrication of nanomaterials", *Europ. Polym. J.* **47**, 584 – 599.

Nguyen, M. N., Bressy, C., and Margaillan, A. (**2009**). "Synthesis of novel random and block copolymers of tert-butyldimethylsilyl methacrylate and methyl methacrylate by RAFT polymerization", *Polymer* **50**, 3086 - 3094.

Park, C., Yoon, J., and Thomas, E. L. (**2003**). "Enabling nanotechnology with self assembled block copolymer patterns", *Polymer* **44**, 6725 - 6760.

Pospiech, D., Werner (Ptacek), S., Jehnichen, D., Komber, H., Friedel, P., Reuter, U., Funari, S. S., Perlich, J., and Voit, B. (**2012**). „Multifunctionalized methacrylate di- and triblock copolymers: Synthesis and nanostructure", *J. Nanostruct. Polym. Nanocomp.* **8**, 58 - 66.

Quirk, R. P., Ocampo, M., Polce, M. J., and Wesdemiotis, C. (**2007**). "Functionalization of Poly(styryl)lithium with Thiiranes: Sulfur Extrusion vs Ring-Opening Mechanisms", *Macromolecules* **40**, 2352 - 2360.

Segalman, R. A. (**2005**). "Patterning with block copolymer thin films", *Mat. Sci. Eng. R* **48**, 191 - 226.

Sepe, A., Cernoch, P., Stepanek, P., Hoppe, E. T., and Papadakis, C. M. (**2014**). "Creation of lateral structures in diblock copolymer thin films during vapor uptake and subsequent drying - effect of film thickness", *Eur. Polym. J.* **50**, 87-96.

Roth, S. V., Döhrmann, R., Dommach, M., Kuhlmann, M., Kröger, I., Gehrke, R., Walter, H., Schroer, C., Lengeler, B., and Müller-Buschbaum, P. (**2006**). "The small-angle options of the upgraded USAXS beamline BW4 at HASYLAB", *Rev. Sci. Instr.* **77**, 085106, 1 - 7.

Taurino, R. (**2008**). "Organic-Inorganic hybrid materials by sol-gel process", PhD Thesis, University of Perugia, Terni (Italy).

Werner, S., Pospiech, D., Jehnichen, D., Eckstein, K., Komber, H., Friedel, P. Janke, A., Näther, F., Reuter, U., Voit, B., Taurino, R., Messori, M. (**2011**). „Synthesis and phase-separation behavior of α,ω-difunctionalized diblock copolymers", *J. Polym. Sci., Part A: Polym. Chem.* **49**, 926 - 937.

Yee, C. K., Jordan, R., Ulman, A., White, H., King, A., Rafailovich, M., and Sokolov, J. (**1999**). "Novel One-Phase Synthesis of Thiol-Functionalized Gold, Palladium, and Iridium Nanoparticles Using Superhydride", *Langmuir* **15**, 3486 - 3491.

Yuan, J., Xu, Y., Walther, A., Bolisetty, S., Schumacher, M., Schmalz, H., Ballauf, M., and Müller, A. H. E. (**2008**). "Water soluble organo-silica hybrid nanowires", *Nature Materials* **7**, 718 - 722.

Zhang, J., Posselt, D., Smilgies, D.-M., Perlich, J., Kyriakos, K., Jaksch, S., and Papadakis, C. M. (**2014**). „Lamellar diblock copolymer thin films during solvent vapor annealing studied by GISAXS: Different behavior of parallel and perpendicular lamellae", *Macromolecules* **47**, 5711 - 5718.